Veterinary Microbiology 232 (2019) 22–29

Contents lists available at ScienceDirect

Veterinary Microbiology

journal homepage: www.elsevier.com/locate/vetmic

In vitro analysis of genetically distinct *Chlamydia pecorum* isolates reveals key growth differences in mammalian epithelial and immune cells

Md. Mominul Islam[a,*], Martina Jelocnik[a], Susan Anstey[a], Bernhard Kaltenboeck[b], Nicole Borel[c], Peter Timms[a], Adam Polkinghorne[d]

[a] Genecology Research Centre, Faculty of Science, Health, Education and Engineering, University of the Sunshine Coast, Sippy Downs, Australia
[b] Department of Pathobiology, Auburn University, Auburn, USA
[c] Institute of Veterinary Pathology, University of Zurich, Switzerland
[d] Animal Research Centre, Faculty of Science, Health, Education and Engineering, University of the Sunshine Coast, Sippy Downs, Australia

ARTICLE INFO

Keywords:
Chlamydia pecorum
In vitro growth
Genetically distinct
Developmental cycle

ABSTRACT

Chlamydia (C.) pecorum is an obligate intracellular bacterium that infects and causes disease in a broad range of animal hosts. Molecular studies have revealed that this pathogen is genetically diverse with certain isolates linked to different disease outcomes. Limited *in vitro* or *in vivo* data exist to support these observations, further hampering efforts to improve our understanding of *C. pecorum* pathogenesis. In this study, we evaluated whether genetically distinct *C. pecorum* isolates (IPA, E58, 1710S, W73, JP-1-751) display different *in vitro* growth phenotypes in different mammalian epithelial and immune cells. In McCoy cells, shorter lag phases were observed for W73 and JP-1-751 isolates. Significantly smaller inclusions were observed for the naturally plasmid-free E58 isolate. *C. pecorum* isolates of bovine (E58) and ovine origin (IPA, W73, JP-1-751) grew faster in bovine cells compared to a porcine isolate (1710S). *C. pecorum* isolates could infect but appear not able to complete their developmental cycle in bovine peripheral neutrophil granulocytes. All isolates, except 1710S, could multiply in bovine monocyte-derived macrophages. These results reveal potentially important phenotypic differences that will help to understand the pathogenesis of *C. pecorum in vivo* and to identify *C. pecorum* virulence factors.

1. Introduction

C. pecorum is an obligate intracellular pathogen with a broad host range. In cattle, sheep, goats and pigs, *C. pecorum* is responsible for several diseases, such as keratoconjunctivitis, polyarthritis, encephalomyelitis and abortion (Longbottom and Coulter, 2003; Walker et al., 2015). Moreover, *C. pecorum* is also considered a common gastrointestinal commensal transmitted by the fecal-oral route with high rates of asymptomatic gastrointestinal tract colonisation reported in both sheep and cattle (Jee et al., 2004). The progression of a primary gastrointestinal tract infection to a systemic infection that results in the characteristic chlamydial diseases in livestock is not understood yet. In other chlamydiae (*C. pneumoniae, C. psittaci* and *C. trachomatis*), it has been suggested that circulating monocytes may help in transferring the bacteria to other organs (Rupp et al., 2009; Ostermann et al., 2013) with different chlamydial species displaying clear phenotypic differences in the ability to infect and/or multiply in peripheral neutrophil granulocytes and/or monocyte-derived macrophages (Koehler et al., 1997; van Zandbergen et al., 2004).

Like other chlamydiae, *C. pecorum* grows intracellularly in eukaryotic cells via a unique bi-phasic developmental cycle. The developmental cycle consists of infectious, metabolically inert and smaller elementary bodies (EBs) and non-infectious, metabolically active and larger reticulate bodies (RBs) (Hackstadt et al., 1997). The developmental cycle starts with attachment to and entry of EBs into host cells. Following endocytosis, the EBs rapidly differentiate into RBs. These RBs divide by binary fission and undergo a sixfold reduction in size within the parasitophorous vacuole and transform back to EBs to be released from the host cell by lysis or extrusion as a completion of developmental cycle (Lee et al., 2018; Hybiske and Stephens, 2008). Interestingly, different *Chlamydia* isolates of the same species exhibit different growth rates *in vitro* which might be correlated to different infection and disease outcomes (Vanrompay et al., 1996). In a mouse genital tract infection model, *C. muridarum* isolates producing large numbers of EBs are associated with high vaginal shedding and more severe pathology compared to isolates which produce less EBs (Lyons et al., 2005).

* Corresponding author at: Genecology Research Centre, Faculty of Science, Health, Education and Engineering, University of the Sunshine Coast, Sippy Downs, 4556, Australia.
E-mail address: mominul.islam@research.usc.edu.au (Md. M. Islam).

https://doi.org/10.1016/j.vetmic.2019.03.024
Received 15 November 2018; Received in revised form 21 February 2019; Accepted 21 March 2019
0378-1135/

Compared to well-studied human chlamydial species *C. trachomatis*, or the murine species *C. muridarum*, much is still to be learned about the biology of *C. pecorum*. Genomic analyses have revealed that *C. pecorum* isolates from koalas, sheep, cattle and pigs share a 1.1 Mbp sized highly conserved and syntenic genome, with any potential genetic variation conferring differences in virulence and tissue and/or host tropism contained to nucleotide variability in the genes encoding for polymorphic membrane proteins (PMPs) and Type III effector (T3SS) proteins, plasticity zone and presence or absence of plasmid (Bachmann et al., 2014; Sait et al., 2014; Jelocnik et al., 2015). Two genetically distinct *C. pecorum* isolates, identified by Multi Locus Sequence Typing (MLST) and designated sequence types ST 23 and ST 69 were described in association with disease in geographically separated sheep flocks and cattle herds in Australia (Jelocnik et al., 2014). More recently, it was proposed that the *C. pecorum* plasmid in plasmid-bearing isolates may contribute to disease development (Jelocnik et al., 2015) given that, in other *Chlamydia* species, it was shown that plasmid-bearing isolates are more infective and are able to induce a more severe pathology in a genital mouse model compared to non-plasmid bearing isolates (O'Connell et al., 2007).

In the following study, we aimed to investigate and compare the *in vitro* growth properties of different genetically distinct *C. pecorum* isolates in a range of mammalian cell types. A range of *in vitro* growth properties were selected to provide further insight into *C. pecorum* cell biology and *in vitro* infection dynamics.

2. Methods

2.1. C. pecorum isolates, cell culture and culture conditions

The characteristics of the five *C. pecorum* isolates used in this study are outlined in Table 1. The genetic identity of each strain was confirmed by amplification of the full-length *C. pecorum ompA* gene (1200 bp) using ompA F 5′ AAGCATAATCTTAGAGGTGAG 3′ and ompA R 5′ CTGTTAGAATCTGCATTGAGC 3′ primers. The amplicons were bidirectionally Sanger sequenced (Macrogen, Korea), following sequence identity analyses using BLAST (https://blast.ncbi.nlm.nih.gov/Blast.cgi). Following a retrieval of MLST profiles for each strain from the PubMLST database (https://pubmlst.org/chlamydiales/), the *ompA* sequences generated in this study were concatenated with the MLST profile of each corresponding strain. The tree was generated with MRBayes using the 4265 bp concatenated sequences alignment as implemented in Geneious v11 (https://www.geneious.com/). We also screened all strains for the detection of chlamydial plasmid. Chlamydial plasmid PCR detection was performed targeting a 233 bp fragment of the *C. pecorum* plasmid CDS5 or *Pgp3* locus, as previously described (Phillips et al., 2018).

All *C. pecorum* isolates were routinely propagated in McCoy cells (CRL-1696, ATCC, USA) at 37 °C, 5% CO_2 in DMEM growth media (Gibco, Australia), supplemented with 5% heat inactivated fetal calf serum (FCS) (Life Technologies, Australia), 120 μg ml^{-1} streptomycin (Sigma-Aldrich, Australia), and 50 μg ml^{-1} Gentamycin (Gibco, Australia). *C. pecorum* isolates were inoculated on McCoy cells with medium supplemented with 1 μg/ml of cycloheximide for 48 h (h). After 48 h post infection (hpi), *C. pecorum* was harvested by mechanical disruption of cells using 3 mm glass beads in Sucrose Phosphate Glutamate (SPG) and stocks were stored at −80 °C until further use. The SPG media consisted of 218 mM sucrose (Sigma-Aldrich, Australia), 3.76 mM KH_2PO_4 (Sigma- Aldrich, Australia), 7.1 mM K_2HPO_4 (Sigma Aldrich, Australia), and 5 mM Glutamic acid (Sigma- Aldrich, Australia), pH, 7.4.

For infection studies, bovine kidney cells (BK) (CCL-22, ATCC, USA), human epithelial cells HEp-2 (CCL-23, ATCC, USA) and murine macrophage cells RAW264.7 (CRL-2278, ATCC, USA) were cultivated in DMEM with 5% FCS, 50 μg/ml gentamicin, 100 μg/ml streptomycin and then infected with the above mentioned isolates as described in 2.3.

2.2. Purification of peripheral blood mononuclear cells (PBMC)

The isolation of PBMCs and growing of monocyte-derived macrophages was performed according to the protocol described elsewhere (Wolf et al., 2005). Briefly, EDTA whole blood were collected from healthy cattle, after approval by the University of the Sunshine Coast Animal Ethics Committee (ANA18135). The whole blood was mixed with sterile PBS (1:1). Five millilitres Ficoll was added to a 15 ml Sepmet tube and combined with 8 ml of the blood/PBS mixture into the Sepmet tube in an upright position. Following centrifugation at 1200xg for 10 min at room temperature, PBMCs were decanted and washed twice in PBS. PBMCs were resuspended in serum-free medium and seeded in a concentration of 3×10^5/ml in 48-well cell culture plates. After 2 h attachment, plates were washed three times with serum-free medium to remove the unbound cells. The attached PMNs cells were grown for 24 h before infection. For macrophage differentiation, bovine monocytes were grown for eight days until they completely converted into monocyte-derived macrophages (Park et al., 2016), with a media change every three days. Macrophage differentiation was confirmed by morphology assessment after staining with Giemsa stain as described elsewhere (Yamaguchi et al., 2002).

2.3. One-step growth curve

For one-step growth curve analysis, 50,000 cells/well of McCoy,

Table 1
Strain information and summary of growth characteristics of the *C. pecorum* isolates used in this study.

Characteristics	*C. pecorum* isolates				
	IPA	**E58**	**1710S**	**W73**	**JP-1-751**
Host	Sheep	Cattle	Pig	Sheep	Sheep
Year of isolation	1968	1940	1969	1989	1968
Isolation tissue	Joints	Brain	Placenta	Intestine	Feces
Country	USA	USA	Austria	Ireland	USA
Clinical manifestation	Polyarthritis	Bovine sporadic encephalomyelitis	Abortion	Asymptomatic	Asymptomatic
ompA genotype[#]	*ompA* 1	*ompA* 1	*ompA* 2	*ompA* 3	*ompA* 1
Sequence Type (ST)	ST48	ST23	ST52	ST68	ST48
Plasmid bearing	Yes	No	No	Yes	Yes
EB initiation time	24 hpi	30 hpi	24 hpi	18 hpi	18 hpi
EB release time	30 hpi	30 hpi	30 hpi	30 hpi	24 hpi
Inclusion size (36 hpi)	16.7 ± 1.03 μm	6.7 ± 0.75 μm	15.7 ± 1.00 μm	15.9 ± 1.44 μm	16.6 ± 1.27 μm
Multiple inclusion	Absent	Absent	Absent	Present	Absent
Inclusion morphology	Irregular lobed	Round	Irregular	Irregular	Irregular lobed

[#] genotype assigned based on nucleotide sequence similarity.

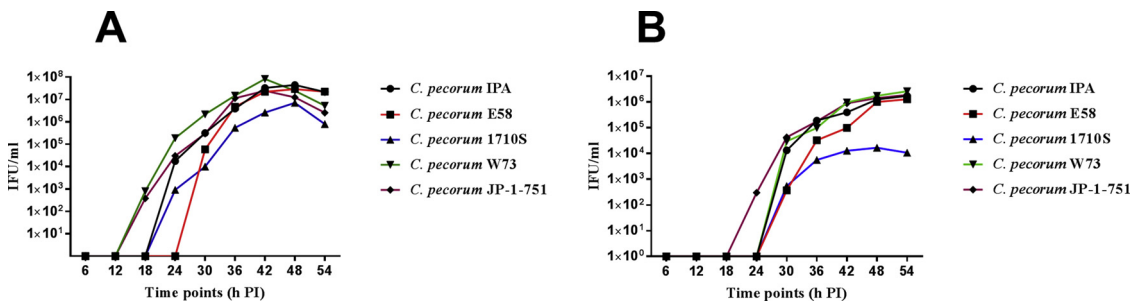

Fig. 1. One-step growth curve of *C. pecorum* IPA, *C. pecorum* E58, *C. pecorum* 1710S, *C. pecorum* W73 and *C. pecorum* JP-1-751 isolates in (A) McCoy cells and (B) release of EB's in extracellular space. Cells were infected at a MOI of 0.3 with the respective isolates, harvested at the described time points and the IFU/ml was determined by sub-passage titration. Each point represents the mean and SD of recoverable IFU/ml from three independent experiments in triplicate.

HEp-2, BK, RAW264.7, PMNs and monocyte-derived macrophages were seeded in 48-well cell culture plates (Sigma Aldrich, Australia) 24 h before infection. At 24 hpi, monolayers were infected at a multiplicity of infection (MOI) of 0.3 and centrifuged for 30 min at 500 x g at 28 °C. At 4 hpi, medium was replaced with fresh medium containing 1 µg/ml of cycloheximide (Sigma Aldrich). The cells were harvested by scraping either at 6 h or 12 h intervals starting at 6 hpi until 54 hpi (6 hpi, 12 hpi, 18 hpi, 24 hpi, 30 hpi, 36 hpi, 42 hpi, 48 hpi, and 54 hpi). Scraped cells stored at −80 °C until determination of infectious titer yield as described elsewhere (Islam et al., 2018).

2.4. Confocal microscopy

McCoy cells were cultured on 8 mm coverslips in a 48-well plate and infected with *C. pecorum* isolates (IPA, E58, 1710S, W73, JP-1-751) at a MOI of 0.3. *Chlamydia* infected cells were fixed with 100% methanol (−20 °C) for 10 min at 16 hpi, 24 hpi and 36 hpi. The coverslips were then washed twice with 1X PBS, pH 7.4. Fluorescein isothiocyanate (FITC) labelled *Chlamydia* lipopolysaccharide (LPS) (Cell labs, Australia) was used to label *Chlamydia* for 45 min coverslips were mounted in glass slides using Prolong Gold antifade (Life Technologies, Australia). Images for morphological observations were captured on a Nikon Eclipse TiS Fluorescent Microscope using a 60 × oil objective. Inclusions sizes (n = 20) at designated time points were determined using the ImageJ software (Islam et al., 2018).

2.5. C. pecorum qPCR assays

The quantification of *C. pecorum* chromosomal DNA was determined by the *C. pecorum* 204bp 16S rRNA gene fragment qPCR assay (Marsh et al., 2011).The qPCRs were performed in a final volume of 20 µl, including 10 µl SYBR Green Quantitect master mix (Qiagen), 1µl of 10 µM each of forward and reverse primer (Easy oligos, Sigma-Aldrich), 3 µl RNAse DNAse free water and 5 µl template DNA. Cycling conditions consisted of 15 min at 95 °C, followed by 35 cycles of 15 s at 94 °C, 15 s at 57 °C and 30 s extension at 72 °C. Negative control (distilled water) and positive control (*C. pecorum* IPA) was included in each assay.

2.6. Statistical analysis

Statistical significance was analysed using unpaired two ways ANOVA test in GraphPad prism (Version 7). $P < 0.05$ were considered significant and results are presented as mean ± standard deviation (SD).

3. Results

3.1. Subtle variations in growth kinetics are present between different C. pecorum isolates in McCoy cells

In a first step, differences in the *in vitro* growth of various *C. pecorum* isolates (IPA, E58, 1710S, W73 and JP-1-751) from different hosts (sheep, cattle, pig) (Table 1) were assessed in McCoy cells. Prior to this, the identity of these isolates was confirmed by amplifying the full length *omp*A gene sequences. The *omp*A sequence analysis revealed the IPA, E58 and JP-1-751 isolates have identical *omp*A genotype (denoted as 1), whereas the 1710S and W73 isolates *omp*A genotypes were respectively denoted genotype 2 and 3, sharing 83.3–88.7% nucleotide identity (Table 1). The phylogenetic tree constructed from an alignment of concatenated full-length *omp*A and MLST sequences, showed that the *C. pecorum* isolates from our study are genetically distinct (Supplementary Fig. 1). In addition, chlamydial plasmid PCR screen performed in this study showed that IPA, W73 and JP-1-751 isolates are plasmid bearing, whilst E58 and 1710S isolates are naturally plasmidless strains.

Initial growth experiments focussed on determining the duration of the chlamydial developmental cycle for each isolate in McCoy cells using one-step growth curves to assess the time required for production of infectious EBs. As shown in Fig. 1A and Table 1, the duration of the developmental cycle to produce infectious *C. pecorum* EBs in McCoy cells varied between *C. pecorum* isolates. Collecting samples at 6 h intervals, we observed that the earliest production (18 hpi) of *C. pecorum* EBs was for the JP-1-751 and W73. At 24 hpi, EBs were present in IPA and 1710S followed by E58 at 30 hpi. While differences between the isolates regarding the duration required for EB production were observed, no major differences could be observed in the yields of *C. pecorum* EBs between 36–48 hpi, with peak EB production detected at 42 hpi for IPA, E58, W73 and JP-1-751 and 48 hpi for the 1710S strain (Fig. 1A).

To further characterise differences in *C. pecorum* EBs production and release, the cell culture media supernatant was collected from each time point and IFU was determined by sub-passage onto cell monolayers. Consistent with the earlier detection of *C. pecorum* JP-1-751 EBs in the one-step growth curve, infectious EBs could be detected in the supernatant of this strain already at 24 hpi, 6 h earlier than for the remaining isolates (30 hpi). The latter observation notably included the W73 isolate in which *C. pecorum* EBs had been detected earlier (at 24 hpi) in the one-step growth curve experiment (Fig. 1B).

In order to know whether the production of infectious progeny paralleled DNA content, we also assessed *C. pecorum* strain growth by using qPCR. Consistent with the one-step growth curve measurements, genome copy numbers gradually increased up to 30 hpi, became linear at 36 and 42 hpi and started declining thereafter (Supplementary Fig. 2).

3.2. Variations in the inclusion morphology observed between C. pecorum isolates

As minor differences in the kinetics of the *C. pecorum* developmental cycle appear to exist between different isolates, we next investigated if any phenotypic differences could be observed in the morphology of the chlamydial inclusions of the different isolates in McCoy cells using LPS staining and confocal microscopy. As shown in Fig. 2, *C. pecorum*

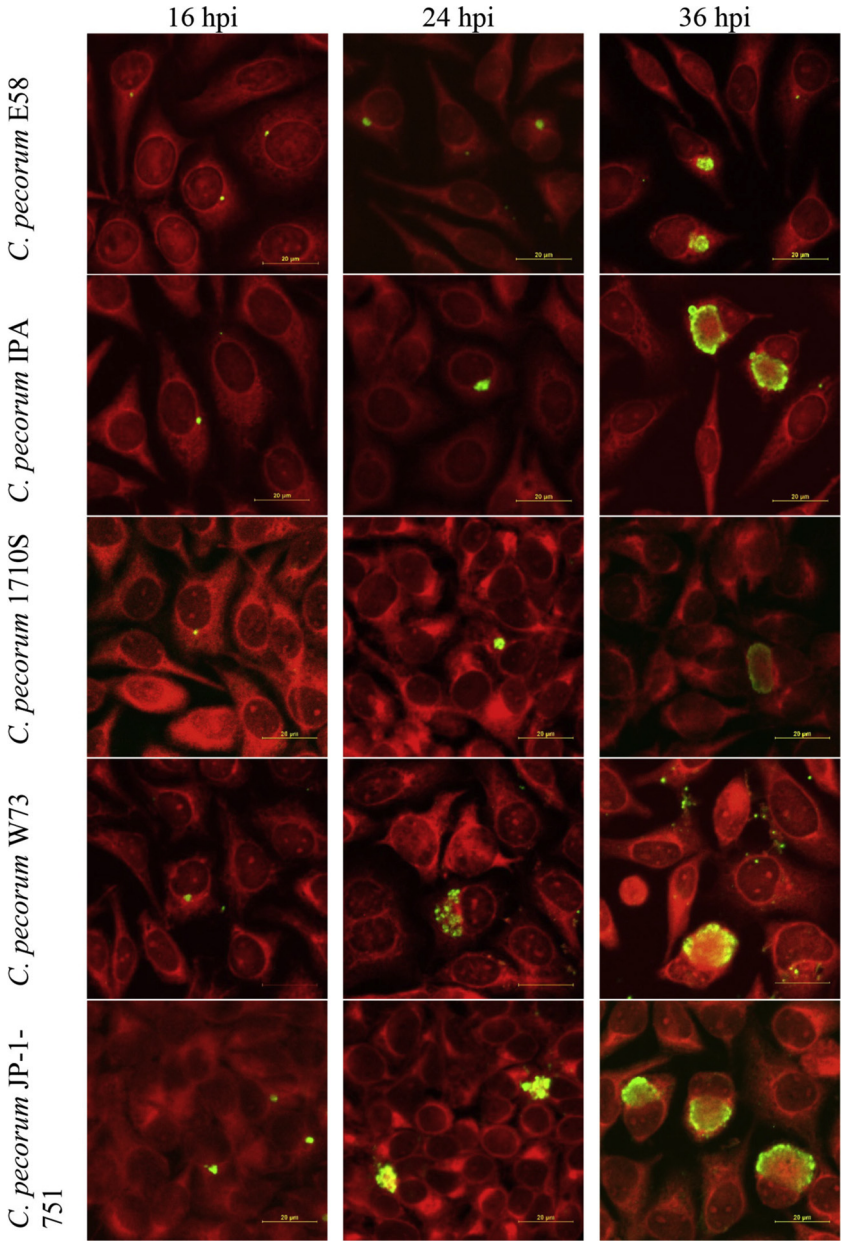

Fig. 2. Confocal microscopic images of *C. pecorum* E58, *C. pecorum* IPA, *C. pecorum* 1710S, *C. pecorum* W73 and *C. pecorum* Jp-1-751 in McCoy cells. Cells were infected at a MOI of 0.3 and fixed at indicated times on the top of panel. *Chlamydia* are shown in green and host cells in red. The scale bar in the bottom right indicates 20 µm. (For interpretation of the references to colour in this figure legend, the reader is referred to the web version of this article).

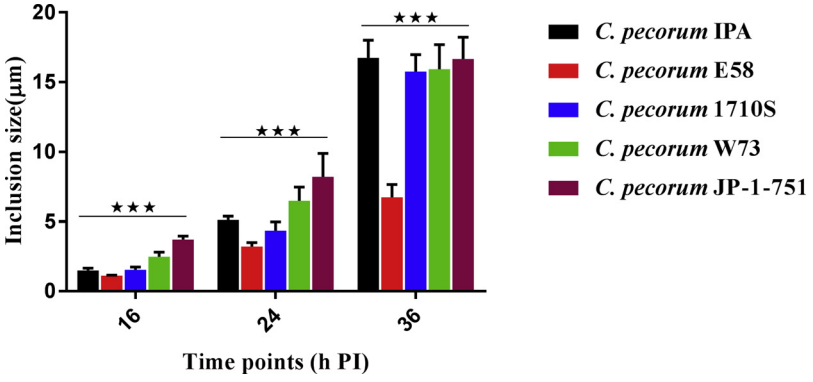

Fig. 3. Inclusion size measurements of *C. pecorum* IPA, *C. pecorum* E58, *C. pecorum* 1710S, *C. pecorum* W73 and *C. pecorum* JP-1-751 in McCoy cells at 16 hpi, 24 hpi and 30 hpi. The inclusion sizes were measured under each condition on three replicate coverslips. The error bar represents SD of the mean of three replicates n = 20. Statistics were determined by two-way ANOVA test, $P < 0.0001$.

inclusions were detected at all three time points (16 hpi, 24 hpi, 36 hpi), consistent with growth curve kinetics. Detailed examination revealed that some isolates exhibited distinct morphological characteristics at the investigated time points. At 16 hpi, inclusions were very small and round for IPA (1.49 ± 0.13 µm), E58 (1.13 ± 0.09 µm), 1710S (1.54 ± 0.16 µm), and W73 (2.4 ± 0.26 µm), whereas larger (3.70 ± 0.21 µm), irregular shaped inclusions were observed only for JP-1-751 (Figs. 2 and 3). The inclusions of all isolates became larger as the developmental cycle progressed at 24 h and 36 hpi (Fig. 3). Multiple inclusions were observed only after infection with the W73 strain. At 36 hpi, the E58 isolate produced significantly smaller (6.74 ± 0.75 µm) and round inclusions compared to the inclusions of other isolates which were irregular in shape with expanding fluorescing lobed areas ($P < 0.001$). Approximately 30% of the IPA (16.73 ± 1.03 µm) and 1710S (15.75 ± 1.00 µm) inclusions formed lobes which became more visible at 36 hpi (Fig. 3).

3.3. *C. pecorum* growth in mammalian epithelial cell lines from different hosts

C. pecorum has one of the broadest host range of chlamydial species currently described in the genus *Chlamydia*. To examine whether the subtle differences in the duration of the *C. pecorum* developmental cycle observed in this initial experiment were specific to McCoy cells, we also investigated the duration of the developmental cycle for all isolates in HEp-2 (Fig. 4A) and BK cell lines (Fig. 4B). In HEp-2 cells, the JP-1-751 isolate showed a 6 h delayed differentiation of RBs to EBs than that observed in the McCoy cell infection experiment. *C. pecorum* EB yield for the JP-1-751 strain was also much lower (< 20%) compared to McCoy cells (Fig. 4A). The timepoint of the first *C. pecorum* EB production in HEp-2 cells was otherwise consistent for all other isolates and comparable to infection in McCoy cells (Fig. 4A). With the exception of the *C. pecorum* 1710S isolate, similar growth kinetics in BK cells could be observed to those seen in the McCoy cell experiments (Fig. 4B). For the 1710S strain, EB production was delayed by 6 h in BK cells compared to McCoy and HEp-2 cell growth experiments with a concomitant reduction in IFU/ml at 54 hpi.

3.4. *C. pecorum* isolates can infect and survive in immune cells

It has been shown for *C. pneumoniae* (Wolf et al., 2005) that circulating or tissue-resident immune-derived cells (alveolar macrophages) are permissive to infection and/or replication. Therefore, we tested the ability of five *C. pecorum* isolates to infect different immune cells. Initial infection experiments focussed on the permissiveness of murine RAW264.7 macrophages to *C. pecorum*. Development of chlamydial inclusions was assessed by confocal microscopy at 36 hpi showing the presence of inclusions in all five *C. pecorum* isolates (Fig. 5A), however, inclusion size was significantly ($p < 0.005$, Student's t test, $n = 3$) smaller for all isolates compared to the inclusions observed previously in McCoy cells (Fig. 5Aa). To assess the duration of the developmental cycle and to quantify infections progeny, one-step growth curves were performed with sampling timepoints at 12 hpi, 24 hpi, 36 hpi and 48 hpi. Chlamydial EBs were detected at 24 hpi for the IPA, 1710S, W73 and JP-1-751 isolates (Fig. 5Ba) and, consistent with our McCoy cell experiments, the E58 isolate lagged behind the others with EBs first detectable at 36 hpi. At 48 hpi, the mean titre of all five *C. pecorum* isolates was significantly lower ($p < 0.005$, Student's t test, $n = 3$) than the IFU recovered from the previously performed McCoy cell infection experiments (10^5 IFU/ml c.f. 10^7 IFU/ml).

Since we had observed subtle differences in the *in vitro* growth kinetics of the *C. pecorum* isolates in mammalian epithelial cells, we then investigated whether *C. pecorum* could infect immune cells derived from one of their natural hosts (cattle). To achieve this, PBMCs were isolated from fresh bovine blood and infected with the five *C. pecorum* isolates. Chlamydial morphology was monitored by immunofluorescence detection of chlamydial inclusions by confocal microscopy at 36 hpi. Fig. 5Ab shows that *C. pecorum* were taken up by the PMNs and intracellular inclusions were detected in PMNs. However, the size of the inclusions was smaller than in the McCoy cells (data not shown). One-step growth curves of similarly infected cells also failed to detect any production of infectious *C. pecorum* EBs in any of the isolates (Fig. 5Bb). To further investigate the potential for chlamydial replication, we performed *C. pecorum*-specific qPCR on samples collected at 0 hpi and 24 hpi for each isolate. Interestingly, chlamydial DNA copy numbers were increased at 24 hpi for all isolates except 1710S (Supplementary Fig. 3), despite the lack of chlamydial replication evidence as assessed by titration experiments.

In contrast, when macrophages derived from these freshly isolated bovine PBMCs were infected, large *C. pecorum* inclusions could be readily detected at 36 hpi for all isolates except for *C. pecorum* 1710S (Fig. 5Ac). This observation was confirmed by the failure to detect any EBs from this isolate (1710S) during subsequent one-step growth curve experiments with sampling timepoints at 12, 24, 36 and 48 hpi (Fig. 5Bc). Interestingly, for the remaining isolates, while the inclusion sizes were similar to those observed in the McCoy cell experiments, the mean titres of recovered IFUs were significantly lower compared to the infection experiments in McCoy cells ($P < 0.0001$; Student's t test, $n = 3$).

4. Discussion

Despite the obvious health impacts that *C. pecorum* infection has on a broad range of animal hosts, our knowledge on the pathogenesis of *C. pecorum*-related diseases is still very limited. In the present study, we determined the *in vitro* growth properties of five genetically diverse *C. pecorum* isolates isolated from different anatomical sites of sheep, cattle or pigs, in different mammalian epithelial and immune cell lines.

A growth curve, including multiple sampling points throughout the developmental cycle, is an option to identify subtle differences in the

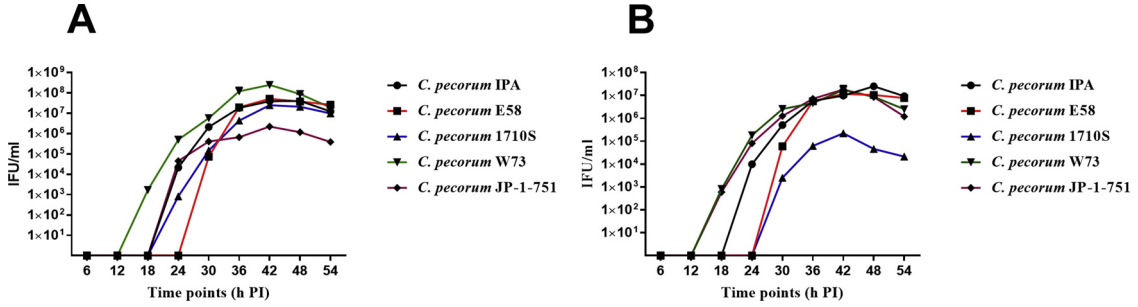

Fig. 4. One-step growth curve of *C. pecorum* IPA, *C. pecorum* E58, *C. pecorum* 1710S, *C. pecorum* W73 and *C. pecorum* JP-1-751 isolates in (A) HEp-2 and (B) BK cells. Cells were infected at a MOI of 0.3 with the respective isolates, harvested at the described time points and the IFU/ml was determined by sub-passage titration. Each point represents the mean and SD of recoverable IFU/ml from three independent experiments in triplicate.

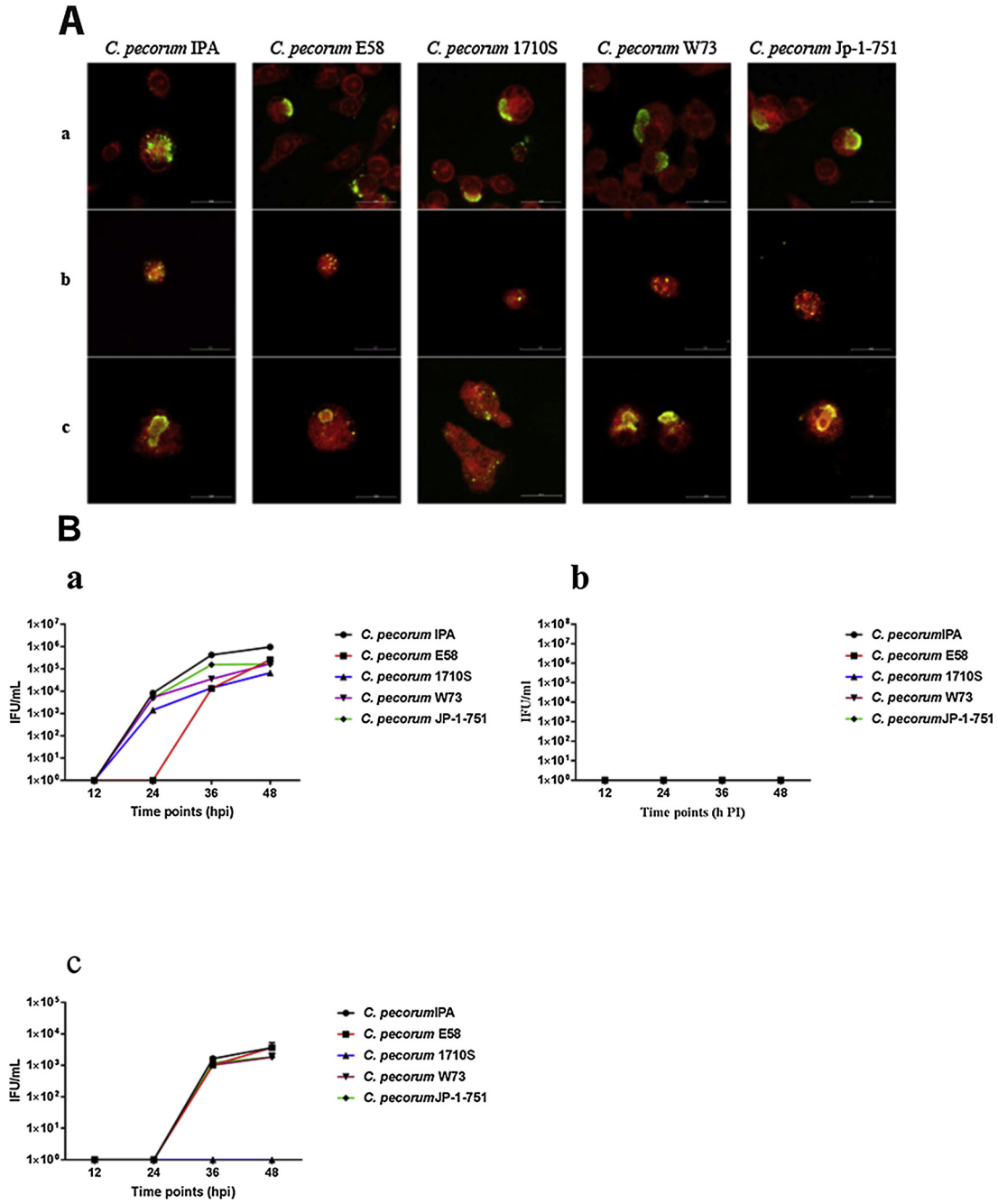

Fig. 5. *C. pecorum* in vitro growth characteristic in RAW264.7 cells. (A) Confocal microscopic images of *C. pecorum* IPA, *C. pecorum* E58, *C. pecorum* 1710S, *C. pecorum* W73 and *C. pecorum* Jp-1-751 in.(a) RAW264.7, (b) PMN's and (c) monocyte derived macrophages. Cells were infected at a MOI of 0.3 and fixed at 36 hpi. *Chlamydia* are shown in green and host cells in red. The scale bar in the bottom right indicates 20 µm. (B) One-step growth curve of *C. pecorum* IPA, *C. pecorum* E58, *C. pecorum* 1710S, *C. pecorum* W73 and *C. pecorum* JP-1-751 isolates in (a) RAW264.7 cells, (b) PMN's, and (c) monocyte derived macrophages. Cells were infected at a MOI of 1.0 with the respective isolates, harvested at the described time points and the IFU/ml was determined by sub-passage titration. Each point represents the mean and SD of recoverable IFU/ml from three independent experiments in triplicate. (For interpretation of the references to colour in this figure legend, the reader is referred to the web version of this article).

growth of isolates from the same chlamydial species over time (Skilton et al., 2018). In this study, we observed subtle differences in the *C. pecorum* developmental cycle at the critical timepoints of RB/EB conversion and release of infective EBs. We found that RB/EB conversion appeared to be initiated earlier for the JP-1-751 and W73 isolates compared to other isolates, suggesting that these isolates completed their developmental cycle earlier than the other isolates. The detailed mechanism that accounts for RB/EB conversion among the strains remain largely unknown. A recent study describes that size of the RB reduced during the continuation of the development cycle of *C. trachomatis* and RB/EB conversion only starts after six rounds of replication (Lee et al., 2018). Furthermore, the JP-1-751 strain released EBs in the media 6 h earlier than other isolates. These differences were also noted previously and described for other cattle and sheep *C. pecorum* isolates, where inclusions were detected 18 to 20 h after infection commenced (Spears and Storz, 1979). We also noted differences in the inclusion morphology of isolates used in our study in McCoy cells. Our results confirmed the irregular shaped inclusion morphology for *C. pecorum* 1710S as reported previously (Schiller et al., 2004). This irregular shaped inclusion might be formed due to the fusion of smaller

inclusions, perhaps as a result of the secretion of type III effectors that might help such homotypic fusions of infected *Chlamydia*-containing vesicles. We also observed multiple inclusions for W73 and a lobular appearance of the inclusions for the IPA and JP-1-751 isolates. Multiple inclusions may form either by infection of cells with multiple EB's or the division of existing inclusions (Matsumoto et al., 1991) which might be associated with niche adapatation or adherence to host cell (Mitchell et al., 2009). It has been shown for *C. pneumoniae* LPCoLN (koala isolate) and *C. psittaci* GPIC that the lobular appearance of the inclusion results from partial fusion of smaller inclusions (Rockey et al., 1996; Mitchell et al., 2009).

The experimental evidence linking *in vitro* growth differences to the *in vivo* pathogenesis has been much better studied in other chlamydial species than in *C. pecorum*. In the absence of comparative *in vivo* data, available genetic data for some of these isolates might be informative, in particular related to the presence of a plasmid. This study revealed that the *C. pecorum* E58 and 1710S strains, unlike IPA, W73 and JP-1-751, does not appear to contain a plasmid. The chlamydial plasmid is in general considered to be a key virulence factor that is present in most chlamydial species (Liu et al., 2014). Extensive plasmid analyses in *C. trachomatis* (Sigar et al., 2014) and *C. muridarum* (Lei et al., 2014) have shown that its loss has a significant impact on the *in vitro* and *in vivo* growth and pathogenicity of *Chlamydia*. *C. muridarum* plasmid-cured isolates show significantly smaller inclusions and have a 4 h developmental delay in growth compared to wild-type isolates (Skilton et al., 2018). Related to the latter finding, the *C. pecorum* E58 strain in our study had a 6 h delay in EB production compared to the other isolates and its inclusions were significantly smaller in McCoy cells. The plasmid function in *C. pecorum* is currently unknown. It is highly distributed in *C. pecorum* isolates from different hosts but apparently not essential to growth (Jelocnik et al., 2015). Ultimately, unravelling the function of the *C. pecorum* plasmid will be only possible by its depletion and/or mutagenesis, followed by detailed *in vitro* and *in vivo* phenotypic comparisons as achieved in other chlamydial species (O'Connell et al., 2007; Skilton et al., 2018).

Another interesting observation was that the porcine *C. pecorum* strain 1710S could not readily infect and grow in both bovine epithelial and immune cells, although genetic evidence suggested that certain isolates can infect the same host (e.g. cattle, sheep and koalas). Interestingly, the genetic analysis performed to date suggests that the porcine isolates are genetically distinct from other isolates sequenced from other hosts such as cattle, sheep and koalas (Jelocnik et al., 2015). Although further analysis of *C. pecorum* porcine isolates is required, it is possible that the porcine isolates represent a distinct biovar of this diverse veterinary pathogen. If so, further genetic analyses of these isolates may prove useful to understanding the factors that define host specificity for *C. pecorum*.

C. pecorum-related diseases such as arthritis and conjunctivitis are hypothesized to result from systemic infection and dissemination from a primary infection in the gastrointestinal tract. The mechanism of this dissemination is currently unclear but may be via the haematogenous route. In the present study, we showed for the first time that *C. pecorum* isolates can infect and survive in different immune cells. Atypical *C. pecorum* inclusions were frequently found in bovine PMNs but we did not observe any infectious progeny in primary PMNs. The reason for this remains unclear but it is possible that conversion of RBs to EBs may be inhibited in monocytes while they (potentially) remain viable. *C. pecorum* infected PMNs may serve as a vehicle to transport infectious particles to epithelial cells, as has been reported for *C. pneumoniae* previously (van Zandbergen et al., 2004). Indeed, *C. pneumoniae* developmental stages protected in monocytes also facilitated engulfment and viability in macrophages (Rupp et al., 2009). Here we showed that *C. pecorum* is able to survive and replicate within the murine macrophage and, at least to some extent, in primary bovine monocyte derived macrophages. The successful replication of *Chlamydia* within macrophages mainly depends on adaptation to the acidic environment in the phagosome and avoidance of fusion with the lysosome. Wolf et al. (2005) reported degradation of *C. pneumoniae* in phagosomes by proteolytic enzyme activity, however, a small proportion could escape this destructive process to complete their developmental cycle. In our study, we also noted that some of the *C. pecorum* inclusions matured in macrophages from bovine and murine hosts by the presence of large inclusions in these cells and the recovery of viable infectious progeny. Whether the infection of *C. pecorum* in macrophages actually occurs in vivo awaits further investigations, however, there is evidence for other *Chlamydia* suggesting that this might be possible (Haranaga et al., 2003). Further work will be required to reveal the role of hematogenous dissemination during *C. pecorum* infections.

In conclusion, this study investigating five *C. pecorum* isolates from different hosts/disease presentations revealed distinct *in vitro* growth phenotypes and, for the first time, the ability of this pathogen to infect and survive in host immune cells. Future investigations should include (a) the use of *in vitro* studies paired with chlamydial genetics systems and genomics to identify the key genes responsible for these *in vitro* phenotypes; and (b) *in vivo* studies of isolates with different growth characteristics to investigate whether the *in vitro* phenotypes have an impact *in vivo*.

Conflict of interest

The authors declare they have no competing interests.

Acknowledgements

We thank Tamieka Fraser for assistance with *Chlamydia* cell culture. This project was funded by an Australian Research Council Linkage Project Grant (LP140100315) awarded to AP.

Appendix A. Supplementary data

Supplementary material related to this article can be found, in the online version, at doi:https://doi.org/10.1016/j.vetmic.2019.03.024.

References

Bachmann, N.L., Fraser, T.A., Bertelli, C., Jelocnik, M., Gillett, A., Funnell, O., Flanagan, C., Myers, G.S.A., Timms, P., Polkinghorne, A., 2014. Comparative genomics of koala, cattle and sheep isolates of Chlamydia pecorum. BMC Genomics 15, 667.

Hackstadt, T., Fischer, E.R., Scidmore, M.A., Rockey, D.D., Heinzen, R.A., 1997. Origins and functions of the chlamydial inclusion. Trends Microbiol. 5, 288–293.

Haranaga, S., Yamaguchi, H., Ikejima, H., Friedman, H., Yamamoto, Y., 2003. *Chlamydia pneumoniae* infection of alveolar macrophages: a model. J. Infect. Dis. 187, 1107–1115.

Hybiske, K., Stephens, R.S., 2008. Exit strategies of intracellular pathogens. Nat. Rev. Microbiol. 6, 99–110.

Islam, M.M., Jelocnik, M., Huston, W.M., Timms, P., Polkinghorne, A., 2018. Characterization of the in vitro *Chlamydia pecorum* response to gamma interferon. Infect. Immun. 86, e00717–17.

Jee, J., Degraves, F.J., Kim, T., Kaltenboeck, B., 2004. High prevalence of natural *Chlamydophila* species infection in calves. J. Clin. Microbiol. 42, 5664–5672.

Jelocnik, M., Walker, E., Pannekoek, Y., Ellem, J., Timms, P., Polkinghorne, A., 2014. Evaluation of the relationship between *Chlamydia pecorum* sequence types and disease using a species-specific multi-locus sequence typing scheme (MLST). Vet. Microbiol. 174, 214–222.

Jelocnik, M., Bachmann, N.L., Kaltenboeck, B., Waugh, C., Woolford, L., Speight, K.N., Gillett, A., Higgins, D.P., Flanagan, C., Myers, G.S., Timms, P., Polkinghorne, A., 2015. Genetic diversity in the plasticity zone and the presence of the chlamydial plasmid differentiates *Chlamydia pecorum* isolates from pigs, sheep, cattle, and koalas. BMC Genomics 16, 893.

Koehler, L., Nettelnbreker, E., Hudson, A.P., Ott, N., Gerard, H.C., Branigan, P.J., Schumacher, H.R., Drommer, W., Zeidler, H., 1997. Ultrastructural and molecular analyses of the persistence of *Chlamydia trachomatis* (serovar K) in human monocytes. Microb. Pathog. 22, 133–142.

Lee, J.K., Enciso, G.A., Boassa, D., Chander, C.N., Lou, T.H., Pairawan, S.S., Guo, M.C., Wan, F.Y.M., Ellisman, M.H., Sutterlin, C., Tan, M., 2018. Replication-dependent size reduction precedes differentiation in Chlamydia trachomatis. Nat. Commun. 9, 45.

Lei, L., Chen, J., Hou, S., Ding, Y., Yang, Z., Zeng, H., Baseman, J., Zhong, G., 2014. Reduced live organism recovery and lack of hydrosalpinx in mice infected with plasmid-free Chlamydia muridarum. Infect. Immun. 82, 983–992.

Liu, Y., Huang, Y., Yang, Z., Sun, Y., Gong, S., Hou, S., Chen, C., Li, Z., Liu, Q., Wu, Y.,

Baseman, J., Zhong, G., 2014. Plasmid-encoded Pgp3 is a major virulence factor for *Chlamydia muridarum* to induce hydrosalpinx in mice. Infect. Immun. 82, 5327–5335.
Longbottom, D., Coulter, L.J., 2003. Animal chlamydioses and zoonotic implications. J. Comp. Pathol. 128, 217–244.
Lyons, J.M., Morre, S.A., Airo-Brown, L.P., Pena, A.S., Ito, J.I., 2005. Comparison of multiple genital tract infections with *Chlamydia trachomatis* in different isolates of female mice. J. Microbiol. Immunol. Infect. 38, 383–393.
Marsh, J., Kollipara, A., Timms, P., Polkinghorne, A., 2011. Novel Molecular marker of *C. Pecorum* genetic diversity in the Koala (*Phascolarctos cinereus*). BMC Microbiol. 11:77.
Matsumoto, A., Bessho, H., Uehira, K., Suda, T., 1991. Morphological studies of the association of mitochondria with chlamydial inclusions and the fusion of chlamydial inclusions. J. Elect. Micros. 40, 356–363.
Mitchell, C.M., Mathews, S.A., Theodoropoulos, C., Timms, P., 2009. In vitro characterisation of koala *Chlamydia pneumoniae*: morphology, inclusion development and doubling time. Vet. Microbiol. 136, 91–99.
O'Connell, C.M., Ingalls, R.R., Andrews, C.W.Jr., Scurlock, A.M., Darville, T., 2007. Plasmid-deficient *Chlamydia muridarum* fail to induce immune pathology and protect against oviduct disease. J. Immunol. 179, 4027–4034.
Ostermann, C., Ruttger, A., Schubert, E., Schrodl, W., Sachse, K., Reinhold, P., 2013. Infection, disease, and transmission dynamics in calves after experimental and natural challenge with a bovine *Chlamydia psittaci* isolate. PLoS One 8 (5) e64066.
Park, K.T., ElNaggar, M.M., Abdellrazeq, G.S., Bannantine, J.P., Mack, V., Fry, L.M., Davis, W.C., 2016. Phenotype and function of CD209+ bovine blood dendritic cells, monocyte-derived-Dendritic cells and monocyte-derived macrophages. PLoS One 11, e0165247.
Phillips, S., Robbins, A., Loader, J., Hanger, J., Booth, R., Jelocnik, M., et al., 2018. *Chlamydia pecorum* gastrointestinal tract infection associations with urogenital tract infections in the koala (Phascolarctos cinereus). PLoS One 13 (11) e0206471.
Rockey, D.D., Fischer, E.R., Hackstadt, T., 1996. Temporal analysis of the developing *Chlamydia psittaci* inclusion by use of fluorescence and electron microscopy. Infect. Immun. 64, 4269–4278.
Rupp, J., Pfleiderer, L., Jugert, C., Moeller, S., Klinger, M., Dalhoff, K., Solbach, W., Stenger, S., Laskay, T., van Zandbergen, G., 2009. *Chlamydia pneumoniae* hides inside apoptotic neutrophils to silently infect and propagate in macrophages. PLoS One 4, e6020.
Sait, M., Livingstone, M., Clark, E.M., Wheelhouse, N., Spalding, L., Markey, B., Magnino, S., Lainson, F.A., Myers, G.S., Longbottom, D., 2014. Genome sequencing and comparative analysis of three *Chlamydia pecorum* isolates associated with different pathogenic outcomes. BMC Genomics 15, 23.
Schiller, I., Schifferli, A., Gysling, P., Pospischil, A., 2004. Growth characteristics of porcine chlamydial isolates in different cell culture systems and comparison with ovine and avian chlamydial isolates. Vet. Journal. 168, 74–80.
Sigar, I.M., Schripsema, J.H., Wang, Y., Clarke, I.N., Cutcliffe, L.T., Seth-Smith, H.M., Thomson, N.R., Bjartling, C., Unemo, M., Persson, K., Ramsey, K., 2014. Plasmid deficiency in urogenital isolates of *Chlamydia trachomatis* reduces infectivity and virulence in a mouse model. Pathog. Dis. 70, 61–69.
Skilton, R.J., Wang, Y., O'Neill, C., Filardo, S., Marsh, P., Benard, A., Thomson, N.R., Ramsey, K.H., Clarke, I.N., 2018. The *Chlamydia muridarum* plasmid revisited : new insights into growth kinetics. Wellcome Open Res. 3, 25.
Spears, P., Storz, J., 1979. Biotyping of *Chlamydia psittaci* based on the inclusion morphology and response to diethylaminoethyl-dextran and cycloheximide. Infec. Immun. 24, 224–232.
van Zandbergen, G., Gieffers, J., Kothe, H., Rupp, J., Bollinger, A., Aga, E., Klinger, M., Brade, H., Dalhoff, K., Maass, M., Solbach, W., Laskay, T., 2004. *Chlamydia pneumoniae* multiply in neutrophil granulocytes and delay their spontaneous apoptosis. J. Immunol. 172, 1768–1776.
Vanrompay, D., Charlier, G., Ducatelle, R., Haesebrouck, F., 1996. Ultrastructural changes in avian *Chlamydia psittaci* serovar A-, B-, and D-infected buffalo green monkey cells. Infect. Immun. 64, 1265–1271.
Walker, E., Lee, E.J., Timms, P., Polkinghorne, A., 2015. *Chlamydia pecorum* infections in sheep and cattle: a common and under-recognised infectious disease with significant impact on animal health. Vet, Journal. 206, 252–260.
Wolf, K., Fischer, E., Hackstadt, T., 2005. Degradation of *Chlamydia pneumoniae* by peripheral blood monocytic cells. Infect. Immun. 73, 4560–4570.
Yamaguchi, H., Haranaga, S., Widen, R., Friedman, H., Yamamoto, Y., 2002. *Chlamydia pneumoniae* infection induces differentiation of monocytes into macrophages. Infect. Immun. 70, 2392–2398.